IJMS
Vol 41, No 4, July 2016

Original Article

Effect of Magnetic Fluid Hyperthermia on Implanted Melanoma in Mouse Models

Maryam Heidari[1,2], MS;
Naghmeh Sattarahmady[1,3], PhD;
Sirus Javadpour[4], PhD;
Negar Azarpira[5], PhD;
Hossein Heli[6], PhD;
Alireza Mehdizadeh[1,3], PhD;
Amirhossein Rajaei[7], PhD;
Tahereh Zare[1,2], MS

[1]Department of Medical Physics, School of Medicine, Shiraz University of Medical Sciences, Shiraz, Iran;
[2]Student Research Committee, Shiraz University of Medical Sciences, Shiraz, Iran;
[3]Nanomedicine and Nanobiology Research Center, School of Medicine, Shiraz University of Medical Sciences, Shiraz, Iran;
[4]Department of Materials Science and Engineering, School of Electrical and Computer Engineering, Shiraz University, Shiraz, Iran;
[5]Transplant Research Center, Department of Pathology, Namazee Teaching Hospital, Shiraz University of Medical Sciences, Shiraz, Iran;
[6]Department of Nanomedicine, School of Advanced Medical Sciences and Technologies, Shiraz University of Medical Sciences, Shiraz, Iran;
[7]Department of Electrical and Electronic, School of Electrical and Electronic Engineering, Shiraz University of Technology, Shiraz, Iran

***Correspondence:**
Alireza Mehdizadeh, PhD;
Department of Medical Physics, School of Medicine, Karimkhan-e Zand Avenue, Postal code: 71348-45794, Shiraz, Iran
Tel\Fax: +98 71 32349332
Email: mehdizade@sums.ac.ir
Received: 12 January 2015
Revised: 22 February 2015
Accepted: 15 March 2015

Abstract

Background: Nowadays, magnetic nanoparticles (MNPs) have received much attention because of their enormous potentials in many fields such as magnetic fluid hyperthermia (MFH). The goal of hyperthermia is to increase the temperature of malignant cells to destroy them without any lethal effect on normal tissues. To investigate the effectiveness of cancer therapy by magnetic fluid hyperthermia, $Fe_{0.5}Zn_{0.5}Fe_2O_4$ nanoparticles (FNPs) were used to undergo external magnetic field (f=515 kHz, H=100 G) in mice bearing implanted tumor.

Methods: FNPs were synthesized via precipitation and characterized using transmission electron microscopy (TEM), vibrating sample magnetometer, and Fourier transform infrared. For in vivo study, the mice bearing implanted tumor were divided into four groups (two mice per group), namely, control group, AMF group, MNPs group, and MNPs&AMF group. After 24 hours, the mice were sacrificed and each tumor specimen was prepared for histological analyses. The necrotic surface area was estimated by using graticule (Olympus, Japan) on tumor slides.

Results: The mean diameter of FNPs was estimated around 9 nm by TEM image and M versus H curve indicates that this particle is among superparamagnetic materials. According to histological analyses, no significant difference in necrosis extent was observed among the four groups.

Conclusion: FNPs are biocompatible and have a good size for biomedical applications. However, for MFH approach, larger diameters especially in the range of ferromagnetic particles due to hysteresis loss can induce efficient heat in the target region.

Please cite this article as: Heidari M, Sattarahmady N, Javadpour S, Azarpira N, Heli H, Mehdizadeh A, Rajaei A, Zare T. Effect of Magnetic Fluid Hyperthermia on Implanted Melanoma in Mouse Models. Iran J Med Sci. 2016;41(4):314-321.

Keywords ● Hyperthermia ● Induced ● Nanoparticles ● Magnetic fields ● Melanoma ● Mice

What's Known

- Magnetic fluid hyperthermia by some magnetic nanoparticles and various amounts of magnetic field has shown good results in cancer therapy in animal studies.

What's New

- Although Fe0.5Zn0.5Fe2O4 nanoparticle is a good candidate for other biomedical applications like contrast enhancement in MRI, it does not induce efficient heat under an external magnetic field.

Introduction

Recently, the use of magnetic nanoparticles (MNPs) in medical applications (e.g. magnetic fluid hyperthermia (MFH), magnetic drug delivery, magneto-mechanical actuation of cell surface receptors, magnetic gene transfection, and magnetic resonance imaging (MRI) contrast improvement) has had an upward trend. Hyperthermia with MNPs is a promising modality in the treatment of cancer. The principle of this technique is to destroy cancer cells by heating them up without lethal effects on normal tissues.[1,2] In comparison with other treatment techniques, this technique is a physical therapy with few side effects and it

can be accompanied by other therapies like radiotherapy and chemotherapy to sensitize resistant malignant cells to these therapies.[3,4] There are several strategies to generate heat for hyperthermia treatment. One method is to use MNPs followed by alternating magnetic field (AMF).[5] Effectiveness of the treatment is dependent on the tumor size and its location in the body. MNPs, used as heating mediators, are magnetic materials consisting of one or more inorganic crystals. When they undergo external magnetic field, thermal energy is dissipated because of Neel and Brownian relaxations and hysteresis losses.[2,6]

The heating power of MNPs depends on the particle size, size distribution, domain state, magnetic anisotropy, the viscosity of the dispersion medium and parameters of the magnetic field, including field strength (H) and frequency (f).[6-8]

Survival of the malignant cells declines when their temperature reaches 41 to 46 °C.[9] In this technique, it is therefore necessary to reach temperatures above 41 °C by MNPs as the heat sources. Tumor cells are more sensitive to heat in comparison to normal cells and consequently these temperatures do not disturb the viability of normal cells.[10]

Dispersing MNPs in a liquid, as a carrier, leads to the production of magnetic fluids. Ferromagnetic iron oxides are the most common MNPs used in biomedical applications. When Fe is substituted by Mn, Co and Zn in $M_{1-x}Zn_xFe_2O_4$ ferrites with superior magnetic properties can be produced.[11]

Several methods are available for synthesizing MNPs, but the most popular methods are coprecipitation, thermal decomposition, hydrothermal synthesis, and laser pyrolysis.[1]

In this study, we synthesized $Fe_{0.5}Zn_{0.5}Fe_2O_4$ ferrite with dextrin coating by the aqueous precipitation method. The samples were characterized by transmission electron microscopy (TEM) to investigate the size distribution and morphology of the nanostructure. Magnetic properties and hysteresis loop of the MNPs were studied by vibrating sample magnetometer (VSM). Fourier transform infrared (FT-IR) was also applied to characterize the structure and purity of the compound. Afterwards, we injected these particles intratumorally in mice bearing implanted melanoma cancer to investigate their hyperthermia effect under AMF.

Materials and Methods

Synthesis of $Fe_{0.5}Zn_{0.5}Fe_2O_4$ Ferrite

Ferrite nanoparticles (NPs) were synthesized by the aqueous precipitation route. Briefly, individual metal chloride or sulfate, in an appropriate stoichiometric proportions, was dissolved in a dilute nitric acid (0.1 mol/L HCl) solution and heated to 80 °C. Sodium hydroxide solution (4 mol/L) was prepared separately and heated to 80 °C. The hot nitrate precursor solution was then rapidly mixed with magnetic stirring (final pH of 12.0). The temperature was then increased to 100 °C and stirring continued for 1 hour. This duration is required for crystallization of the ferrites. Then, the solution was cooled and the precipitate was collected by a permanent magnet and washed several times with distilled water to neutralize the supernatant. The ferrite samples were dried at room temperature.

Characterization

TEM (Zeiss, EM10C, 80 kV, Germany) was performed to obtain the morphology and size of the nanostructure. Magnetic properties of ferrofluid were determined by drying the fluid and using a VSM (Meghnatis Kavir Co., Kashan, Iran) at room temperature. Surface structure of the sample was identified by using a FT-IR spectroscope (Burker Tensor 27). The FT-IR spectrum was acquired in the wavenumber range of 500-4000 cm^{-1}.

Cell and Mice Preparation

B16/F10 melanoma cells were purchased from the Pasteur Institute (Iran) and cultured in DMEM (Dulbecco's Modified Eagle Medium) medium with 10% FBS (Fetal Bovine Serum) and 1% penicillin in a humidified 37°C incubator.

Four- to six-week-old inbred BALB/C mice were purchased from the Center of Comparative and Experimental Medicine, Shiraz University of Medical Sciences, Shiraz, Iran. All animals were housed in the laboratory of the Center of Comparative and Experimental Medicine under identical conditions. The animals were housed in special cages at a controlled temperature (24±2 °C) with weekly floor exchange. They had free access to water and standard pelleted laboratory animal diets. A 12:12 hour light-dark cycle was followed in the above-mentioned animal house center. All animals received care in compliance with the Standard Animal Ethics of Iran.

To implant solid tumor, 15×10^5 B16/F10 melanoma cells in PBS were injected subcutaneously into the back of the neck of each mouse. After approximately one week, the tumors appeared and the mice were followed until their tumors reached an appropriate size. To measure the tumor volume, a caliper was used and the volume was computed using the following formula.[12]

$V=0.5\ a\times b^2$ (1)

Where "a" and "b" are the largest and smallest diameter of tumor, respectively. After reaching an appropriate tumor size (about 1 cm^3), hypethermia study was started.

AMF System

In order to generate alternating magnetic field (AMF), a horizontal solenoid coil vibrating 100 G at 515 kHz (sine wave pattern) was used (Shiraz University, School of Engineering). The solenoid had an inner diameter of 5 cm, a length of 15 cm and 14 turns. It consisted of a water-cooling system to avoid heat induction because of the impedance. A resonant H-bridge ZCS inverter with a capacitor bank of 75 nF was employed to derive the coil and inject AC current. Capacitor bank was in series with the solenoid coil, which constitutes the resonant tank. The inverter changed DC input voltage to a square wave alternating voltage and was applied to the resonant tank. Sinusoidal current flowed through the coil while the frequency of the square wave voltage was adjusted to the resonant frequency of the resonant tank. The injected AC current generated AMF whose amplitude was calculated according to the coil characteristics and the magnitude of AC current.

$$B_m = \frac{\mu_0 N I_m}{l} \quad (2)$$

Where, N: Number of turns, l: Coil length, μ_0: Equal to $4\pi*10^{-7}$ and is the magnetic permeability in vacuum, B_m: Peak value of AMF, and I_m: Peak value of AC current.

The peak value of the current was adjusted to 85 A, which was measured using GDS-1072 oscilloscope. The maximum input power of the system was 650 W.

Hyperthermia Experiment

Mice bearing implanted solid tumor in proper conditions were selected and divided into four groups consisting of two mice per group. It included a control group (group A) without any treatment administration and a sham treatment group (group B) to investigate the effect of magnetic field on the malignant cells. The mice in group B were located in the solenoid coil for 30 min without MNPs injection. For evaluating the lethal effects of the FNPs on cancerous cells, the mice in group C received only intratumoral injection of FNPs. Finally, group D was chosen for treatment administration by intratumoral injection of MNPs (200 µl magnetic fluid containing 2 mg Fe) undergoing AMF for 30 min. Intratumoral injection was done to make a desired concentration of MNPs in the tumor. Before administrating the experimental treatment, each mouse was anesthetized with intramuscular injection of Ketamin/Xylazine mix.

Specimen Collection and Histological Analysis

For histological findings, all treated and non-treated tumors and tissues of the spleen, kidney, and liver were removed 24 hours after the treatment. For this purpose, after dissection, the tissues were removed and each specimen was collected and fixed by immersion in 10% buffered formalin and routinely processed into paraffin. Afterwards, sections were cut at 5 µm and put in an oven for 45 minutes to remove the extra paraffin from the tissue. After staining with hematoxylin and eosin (H&E), Perl's iron staining was carried out to obtain the iron content in groups C and D. Finally, each prepared slide was observed under a microscope to distinguish necrosis and inflammation areas and the distribution of MNPs through the track of iron. For this purpose, the necrotic surface area was estimated by using graticule (Olympus, Japan) on tumor slides.

Results

Characterization of Nanoparticles

Magnetic properties of NPs were determined by vibrating sample magnetometer (VSM) at room temperature. Figure 1 depicts the M versus H curve of the dry $Fe_{0.5}Zn_{0.5}Fe_2O_4$ ferrite NPs with applied field between -8500 Oe and 8500 Oe at room temperature. Figure 2 illustrates the size distribution of NPs. As shown in this figure, the particle size, morphology, and agglomeration of MNPs can be determined by TEM images.

In order to confirm that dextrin was successfully coated on the surface of NPs, FT-IR analysis was done. Figure 3 shows the FT-IR spectra of dextrin-coated FNPs.

Hyperthermia Experiment

For the in vivo study, the tumor was induced in BALB/C mice via the injection of B16/F10 melanoma cells in PBS into the back of the neck of the mice. After approximately one week, the tumors appeared in the animals and the size of tumors was measured with a caliper (figure 4).

Figure 5 shows that the mice in groups B and D were located in the center of the solenoid and subjected to AMF with 50 A/div current (figure 6) for 30 minutes.

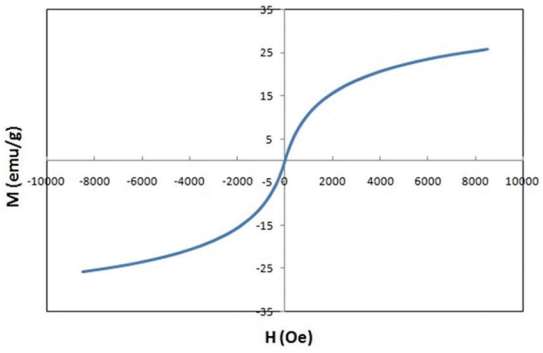

Figure 1: M versus H curve of $Fe_{0.5}Zn_{0.5}Fe_2O_4$ ferrite (at room temperature) indicates the single domain superparamagnetic properties of MNPs.

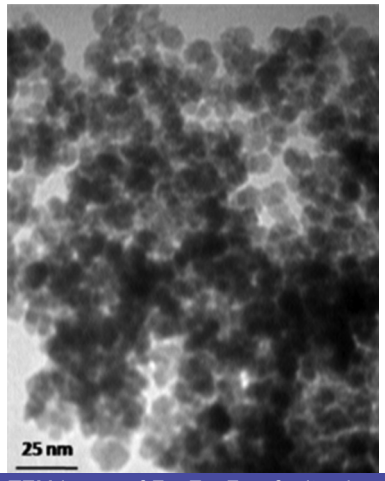

Figure 2: TEM image of $F_{e0.5}Z_{n0.5}F_{e2O4}$ ferrite shows that the diameter of nanoparticles is around 9 nm.

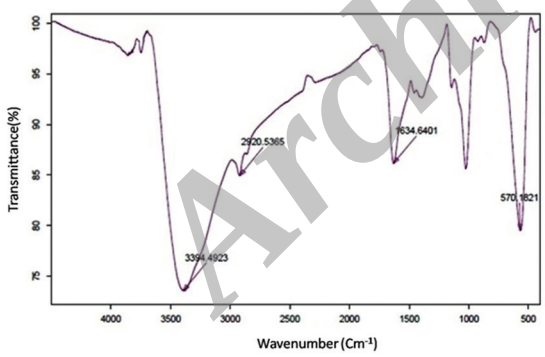

Figure 3: FT-IR spectra of $Fe_{0.5}Zn_{0.5}Fe_2O_4$ ferrite shows NPs were successfully covered with dextrin.

Figure 4: Tumor size was measured by a caliper.

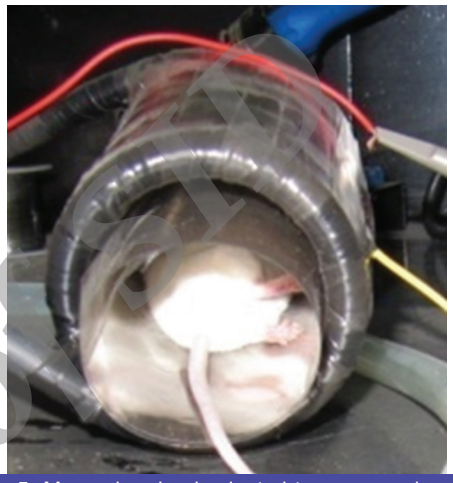

Figure 5: Mouse bearing implanted tumor was placed in a solenoid (f=515 kHz, H=100 G).

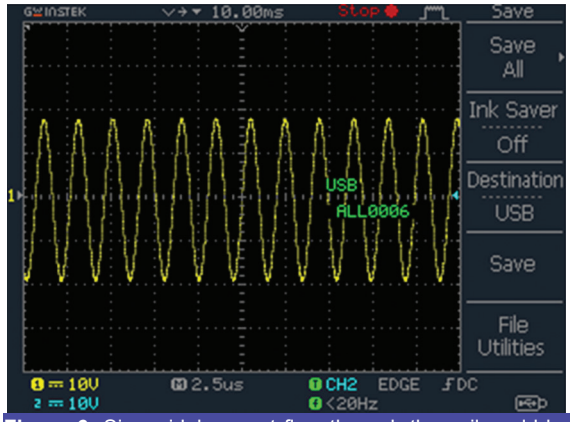

Figure 6: Sinusoidal current flow through the coil could be seen by oscilloscope (50 A/div).

The final aim of this study was to investigate microscopic changes in tumor cells. After 24 hours, all mice were sacrificed and each specimen of the tumors was collected and prepared for histological analyses.

Histological Analysis

Figure 7 shows stained slides of tumors in four groups. In order to document the presence of FNPs between the cells and to investigate their effects on the surrounding medium, Perl's iron staining was done.12,13 As shown in figure 7C, iron particles were present in malignant cells.

No trace of FNPs was detected in the spleen, kidney, and liver tissues and they had normal tissues, figure 8.

Discussion

Due to many side effects of common strategies for cancer therapy, these strategies are not

considered useful for all kinds and stages of tumors. Consequently, researchers are looking for a comprehensive treatment method. One of the potential therapies is local hyperthermia with MNPs. Parameters that contribute to the induction of heat in this technique are the diameter of NPs, anisotropy constant, fluid viscosity, and frequency and amplitude of the magnetic field.[6-8]

In this study, for the characterization of FNPs, FT-IR, VSM, TEM were done. The absence of hysteresis loop in this curve and non-saturated magnetization at the applied magnetic field, indicated the single domain superparamagnetic properties of MNPs.[14]

The experiment magnetic moment (n_b) could be calculated by the following formula.[15]

$$n_b = \frac{M \times M_S}{5585} \quad (3)$$

Where, M is the molecular weight of the composition (in gram), M_s is saturation magnetization, and 5585 is the magnetic factor. By estimating the saturation magnetization through extrapolation (30.16 emu/gr), n_b was calculated to be 1.27.

According to TEM image, the average diameter of the sphere particles was estimated to be 9 nm. For in vivo study, it is necessary to coat the NPs with a polymer. In this study, we used dextrin as a coating for biocompatibility of NPs. FT-IR analysis was used to confirm that dextrin was successfully coated on the surface of MNPs. In FT-IR spectrum, the peak at 570 cm^{-1} refers to the characteristic absorption of Fe-O bond of magnetic particles.[13] The peaks at 1634.6 cm^{-1} and 2920.5 cm^{-1} corresponded to C=O bond and vibration of -CH_2- groups, respectively. A peak at 3394.5 cm^{-1} indicated the presence of hydroxyls on the MNPs surface. Thus, according to previous studies,[16-18] FNPs were successfully covered with dextrin.

In this study, microscopic changes in tumoral cells were investigated 24 hours after treatment among the four mice groups. For this purpose, the degree of necrosis and inflammation (×400) was verified on tumor slides. According to the pathology results, in the tumoral tissue, necrotic cells were easily seen in the central part of all tumors. On tumor slides belonging group C, there was no necrosis cells around NPs. This indicates that FNPs alone do not show any anti-melanoma effect. Thus, it is expected that if FNPs are transferred to other organs in intravenous administration, they do not make lethal effects on the normal cells. However, a previous study[12] showed iron/iron oxide core/shell NPs with porphyrin coating caused cell damage due to the generation of free radicals and magnetic hyperthermia under the influence of magnetic field.

Different degrees of necrotic cells could be seen in all specimens, but no significant difference in necrosis extent was observed among the four groups; thus, this treatment was not powerful enough to remove the cancer cells, which may contribute to particle size.

Three mechanisms contribute to heat loss in MNPs, namely, hysteresis losses, Neel and Brownian relaxations.[6] Bakoglidis et al.[6] investigated the magnetic hyperthermia response of iron oxide NPs in the size range of 5-18 nm. They divided these NPs into three categories; the superparamagnetic (SPM) region (as large as 10 nm) where heating is mainly because of Neel relaxation, the SPM-Ferromagnetic region (10-13 nm), and

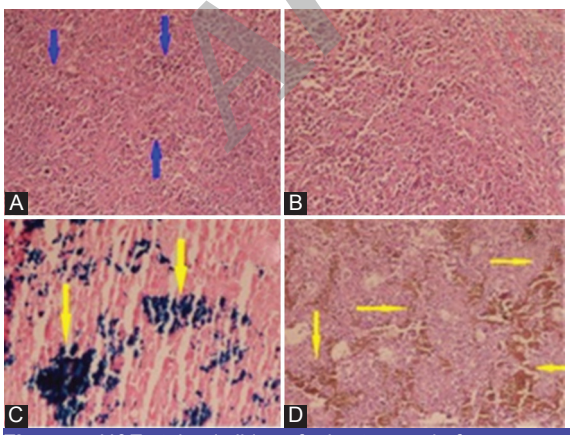

Figure 7: H&E stained slides of mice tumors in four groups. A: Group A (blue arrows show malignant cells); B: Group B; C: Iron stained slide of mouse tumor in group C (yellow arrow shows the presence of Fe nanoparticles in malignant cells); D: H&E stained slide of mouse tumor in group D. No significant difference in the necrosis extent was observed (H&E ×400).

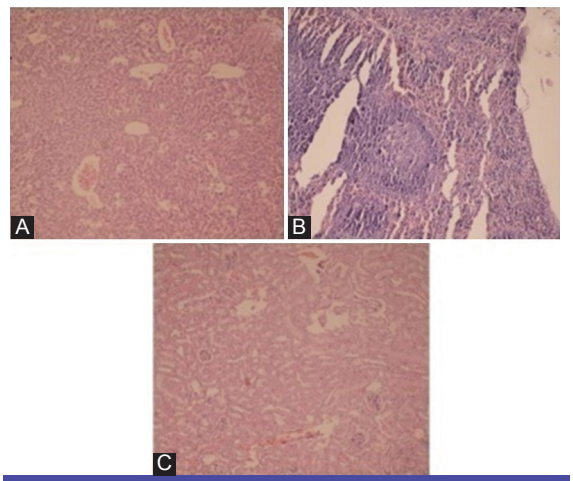

Figure 8: No trace of MNPs was observed in the tissues of the liver (A), spleen (B), and kidney (C) (H&E ×400).

the ferromagnetic region (>13 nm) where hysteresis loss mechanism is dominate in heat dissipation. They reported that ferromagnetic materials release heat that is more significant and hysteresis mechanism is more efficient for hyperthermia applications. In addition, Jeun et al.[19] reported that the heat efficiency of Fe_3O_4 particles below 9.8 nm under 110 kHz magnetic field frequency was insufficient for hyperthermia applications, and the value of specific loss power (SLP) had an upward trend with an increase in the particle size from 11.5 to 22.5 nm under the same magnetic field. Therefore, heat efficiency of FNPs with an average diameter of 9 nm under the influence of AMF (515 kHz) is insufficient for hyperthermia applications. Although, ultra-small NPs have a lot of potential for use in biomedical applications, it was confirmed that this NP could not induce efficient heat for hyperthermia. However, studies[20,21] show the MNP aggregate to larger cluster after systematic administration and therefore the effective hydrodynamic size of the MNP in the body is different from the initial size of NPs. Additionally, theoretical study on proton relaxation indicates that the magnetic properties of NPs increase significantly upon the enhancement of the particle and the crystallite size.[22]

Ultra-small NPs can be functionalized and guided by an external magnetic field for in vivo studies and after removing the EMF, dipoles return to random orientations because of the SPM behavior of these NPs. Unlike ferromagnetic NPs, the embolism in capillary vessels does not occur. However, for the hyperthermia study, SPM NPs show lower heating efficiency than single domain ferromagnetic NPs due to the absence or negligible amounts of hysteresis loss.[6]

We also surveyed the presence of NPs in other organs such as the spleen, kidney, and liver. No trace of FNPs was detected in the spleen, kidney, and liver tissues. Thus, MNPs remained in the tumor and did not transfer to other organs after intratumoral injection. In systemic administration, large particles (>50 nm) are taken up by the liver cells, but smaller ones generally circulate for a longer period. Longer residence time in the blood stream may enhance (enhanced permeation and retention) EPR effect.[12,23] Therefore, it is expected that in systemic administration, FNPs with a diameter of 9 nm are not captured by the liver and accumulated by tumor.

A limitation of this investigation was the use of a solenoid coil with one frequency and field strength. A more equipped device with variable frequency and field strength may give better results.

Conclusion

The major findings reported here illustrate that FNP ferrofluid coated with dextrin is a good candidate for in vivo approaches without any side effects on body organs. While Fe particles were seen in malignant tumor cells, there was no trace of them in other organs. Different amounts of necrosis were seen in the tumor tissues of all groups, but no significant difference in the necrosis extent was observed among the groups. Therefore, although this NP is a good agent for other biomedical applications, like contrast enhancement in MRI, it did not induce efficient heat under external magnetic field.

Acknowledgment

This article was extracted from the thesis written by M. Heidari, under the supervision of Dr. Mehdizadeh and Dr. Sattarahmady. It was financially supported by Shiraz University of Medical Sciences, grants No. 6790. We would like to thank the Research Consultation Center, Shiraz University of Medical Sciences. Animal experiments of this study were supported by the Center of Comparative and Experimental Medicine, Shiraz University of Medical Sciences. The authors would also like to acknowledge Mr. Kouhi, Mrs. Esfandiari and Mr. Shahriari for their contribution to this study.

Conflict of Interest: None declared.

References

1. Doaga A, Cojocariu A, Amin W, Heib F, Bender P, Hempelmann R, et al. Synthesis and characterizations of manganese ferrites for hyperthermia applications. Mater Chem Phys. 2013;143:305-10. doi: 10.1016/j.matchemphys.2013.08.066.
2. Kozissnik B, Bohorquez AC, Dobson J, Rinaldi C. Magnetic fluid hyperthermia: advances, challenges, and opportunity. Int J Hyperthermia. 2013;29:706-14. doi: 10.3109/02656736.2013.837200. PubMed PMID: 24106927.
3. Sun H, Xu L, Fan T, Zhan H, Wang X, Zhou Y, et al. Targeted hyperthermia after selective embolization with ferromagnetic nanoparticles in a VX2 rabbit liver tumor model. Int J Nanomedicine. 2013;8:3795-804. doi: 10.2147/IJN.S50373. PubMed PMID: 24124367; PubMed Central PMCID: PMC3795007.
4. Kut C, Zhang Y, Hedayati M, Zhou H, Cornejo C, Bordelon D, et al.

Preliminary study of injury from heating systemically delivered, nontargeted dextran-superparamagnetic iron oxide nanoparticles in mice. Nanomedicine (Lond). 2012;7:1697-711. doi: 10.2217/nnm.12.65. PubMed PMID: 22830502; PubMed Central PMCID: PMC3991127.

5. Motoyama J, Yamashita N, Morino T, Tanaka M, Kobayashi T, Honda H. Hyperthermic treatment of DMBA-induced rat mammary cancer using magnetic nanoparticles. Biomagn Res Technol. 2008;6:2. doi: 10.1186/1477-044X-6-2. PubMed PMID: 18298831; PubMed Central PMCID: PMC2266920.
6. Bakoglidis K, Simeonidis K, Sakellari D, Stefanou G, Angelakeris M. Size-dependent mechanisms in AC magnetic hyperthermia response of iron-oxide nanoparticles. IEEE Trans Magn. 2012;48:1320-3. doi: 10.1109/TMAG.2011.2173474.
7. Kumar CS, Mohammad F. Magnetic nanomaterials for hyperthermia-based therapy and controlled drug delivery. Adv Drug Deliv Rev. 2011;63:789-808. doi: 10.1016/j.addr.2011.03.008. PubMed PMID: 21447363; PubMed Central PMCID: PMC3138885.
8. Di Barba P, Dughiero F, Sieni E. Magnetic field synthesis in the design of inductors for magnetic fluid hyperthermia. IEEE Trans Magn. 2010;46:2931-4. doi: 10.1109/TMAG.2010.2044769.
9. Bettge M, Chatterjee J, Haik Y. Physically synthesized Ni-Cu nanoparticles for magnetic hyperthermia. Biomagn Res Technol. 2004;2:4. doi: 10.1186/1477-044X-2-4. PubMed PMID: 15132747; PubMed Central PMCID: PMC420488.
10. Pradhan P, Giri J, Rieken F, Koch C, Mykhaylyk O, Doblinger M, et al. Targeted temperature sensitive magnetic liposomes for thermo-chemotherapy. J Control Release. 2010;142:108-21. doi: 10.1016/j.jconrel.2009.10.002. PubMed PMID: 19819275.
11. Pradhan P, Giri J, Samanta G, Sarma HD, Mishra KP, Bellare J, et al. Comparative evaluation of heating ability and biocompatibility of different ferrite-based magnetic fluids for hyperthermia application. J Biomed Mater Res B Appl Biomater. 2007;81:12-22. doi: 10.1002/jbm.b.30630. PubMed PMID: 16924619.
12. Balivada S, Rachakatla RS, Wang H, Samarakoon TN, Dani RK, Pyle M, et al. A/C magnetic hyperthermia of melanoma mediated by iron(0)/iron oxide core/shell magnetic nanoparticles: a mouse study. BMC Cancer. 2010;10:119. doi: 10.1186/1471-2407-10-119. PubMed PMID: 20350328; PubMed Central PMCID: PMC2859385.
13. Zhao Q, Wang L, Cheng R, Mao L, Arnold RD, Howerth EW, et al. Magnetic nanoparticle-based hyperthermia for head & neck cancer in mouse models. Theranostics. 2012;2:113-21. doi: 10.7150/thno.3854. PubMed PMID: 22287991; PubMed Central PMCID: PMC3267386.
14. Köseoğlu Y, Bay M, Tan M, Baykal A, Sözeri H, Topkaya R, et al. Magnetic and dielectric properties of Mn0. 2Ni0. 8Fe2O4 nanoparticles synthesized by PEG-assisted hydrothermal method. J Nanopart Res. 2011;13:2235-44.
15. Hankare P, Patil R, Sankpal U, Jadhav S, Lokhande P, Jadhav K, et al. Investigation of structural and magnetic properties of nanocrystalline manganese substituted lithium ferrites. J Solid State Chem. 2009;182:3217-21. doi: 10.1016/j.jssc.2009.08.034.
16. Varshosaz J, Sadeghi-aliabadi H, Ghasemi S, Behdadfar B. Use of magnetic folate-dextran-retinoic acid micelles for dual targeting of doxorubicin in breast cancer. Biomed Res Int. 2013;2013:680712. doi: 10.1155/2013/680712. PubMed PMID: 24381941; PubMed Central PMCID: PMC3870081.
17. Hong R, Feng B, Chen L, Liu G, Li H, Zheng Y, et al. Synthesis, characterization and MRI application of dextran-coated Fe 3 O 4 magnetic nanoparticles. Biochem Eng J. 2008;42:290-300.
18. Hong R, Li J, Qu J, Chen L, Li H. Preparation and characterization of magnetite/dextran nanocomposite used as a precursor of magnetic fluid. Chem Eng J. 2009;150:572-80. doi: 10.1016/j.cej.2009.03.034.
19. Kolhatkar AG, Jamison AC, Litvinov D, Willson RC, Lee TR. Tuning the magnetic properties of nanoparticles. Int J Mol Sci. 2013;14:15977-6009. doi: 10.3390/ijms140815977. PubMed PMID: 23912237; PubMed Central PMCID: PMC3759896.
20. Tiefenauer LX, Kuhne G, Andres RY. Antibody-magnetite nanoparticles: in vitro characterization of a potential tumor-specific contrast agent for magnetic resonance imaging. Bioconjug Chem. 1993;4:347-52. doi: 10.1021/bc00023a007. PubMed PMID: 8274518.
21. Eberbeck D, Lange A, Hentschel M. Identification of aggregates of magnetic

nanoparticles in ferrofluids at low concentrations. J Appl Crystallogr. 2003;36:1069-74. doi: 10.1107/S002188980301104X.
22. Morales M, Bomati-Miguel O, De Alejo RP, Ruiz-Cabello J, Veintemillas-Verdaguer S, O'Grady K. Contrast agents for MRI based on iron oxide nanoparticles prepared by laser pyrolysis. Journal of Magnetism and Magnetic Materials. 2003;266:102-9. doi: 10.1016/S0304-8853(03)00461-X.
23. Abdeen S, Praseetha P. Diagnostics and treatment of metastatic cancers with magnetic nanoparticles. J Nanomedine Biotherapeutic Discov. 2013;3:115. doi: 10.4172/2155-983X.1000115.